Andreas Theocharis, Thomas Zacharias, Dimitrios Tsanakas, John Milias-Argitis
University of Patras, Patras, Greece

MODELING OF A GRID CONNECTED PHOTOVOLTAIC SYSTEM USING A GEOMETRIAL TRANSFORMER MODEL

Abstract: A grid connected single-phase photovoltaic system is modeled and simulated using a geometrical core-type transformer model. The transformer model that is used takes into account the magnetic core geometry as well as the hysteresis loop of the core material. In particular, the hysteresis loop is introduced using the Jiles-Atherton theory of magnetic hysteresis. Moreover, proper models for the photovoltaic array and the inverter have been used to assemble a system model in the field of state equations. Comparison with published results has been made with a prototype installation of the same configuration. Very good agreement is accomplished between the predicted and measured values. Thus, the proposed methodology can be used for the modeling of single-phase or three-phase grid connected photovoltaic systems.

1. Introduction

The progress being made in the technology of photovoltaic (PV) cells leads to an increased use of grid connected PV systems. The harmonic currents injected into the utility grid may be a serious problem since they could lead to unacceptable levels of wave shapes distortion.

Although the dc-ac inverters are usually based on the PWM method, in this paper a system model for the configuration of a grid connected PV system, Fig. 1, located in Phoenix, Arizona and known as John F. Long PV System is presented [1]-[3]. Specifically, a detailed transformer model is used to represent the transformer that connects the PV installation with the utility grid. Moreover, an incremental model of the PV generator is used to permit a system model in the field of state equations. In the system simulation presented in [1] the transformer is simplified to a linear equivalent inductance and consequently, differences between measured and predicted values have been revealed. Using the proposed system model, simulation results are presented which when compared with measured values found in [1] ensure the validity of the proposed system model.

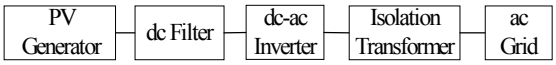

Fig. 1. A block diagram of a possible grid connected PV system

2. Components modeling

2.1. Photovoltaic generator model

The well-known *i-v* non-linear relations describing a PV generator are

$$i_{pv} = I_{ph} - I_o\left[e^{W\left(v_{pv}+i_{pv}r_{sr}\right)} - 1\right] \tag{1}$$

which is an implicit relation or equivalently

$$v_{pv} = -i_{pv}r_{sr} + \frac{1}{W}\ln\left(\frac{I_{ph} - i_{pv}}{I_o} + 1\right) \tag{2}$$

which is an explicit relation, more easily handled mathematically.

In (1) and (2) i_{pv} and v_{pv} are the output current and voltage respectively, r_{sr} is the series resistance, I_{ph} is the light-generated current, I_o is the diode saturation current, $W = q/(wKT_a)$ is the coefficient of the exponential, q is the electron's charge, w is a curve fitting constant, K is the Boltzmann's constant and T_a is the absolute temperature.

In this work, an incremental model of the PV generator is employed [4], [5]. Expanding the $v_{pv}(i_{pv})$ relation (2) in a Taylor series, keeping only the first two terms and defining $r_{dn} = dv_{pv}/di_{pv}\big|_{t=t_n}$ as the incremental resistance of the PV generator one gets

$$v_{pv,n+1} = e_{dn} - r_{dn}i_{pv,n+1} \tag{3}$$

where

$$e_{dn} = v_{pv,n} + r_{dn}i_{pv,n} \tag{4}$$

$$r_{dn} = r_{sr} + \frac{1}{W\left(I_{ph} - I_o - i_{pv,n}\right)} \tag{5}$$

In Fig. 2 this model is shown as an equivalent circuit valid for the time interval $t_n < t < t_n + \Delta t$ (Δt is the time step). In any subsequent time interval one has to update the values of r_{dn}, e_{dn} through relations (2), (4) and (5).

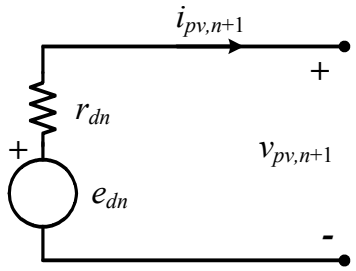

Fig. 2. Incremental model of a PV generator

2.2. Inverter model

The system employs a line-commutated single-phase bridge inverter, Fig. 3. The valves are modeled as ideal switches. Three modes of conduction are considered i.e. none, two or three valves conducting. A four-dimensional state vector **S** is introduced which defines the mode of conduction in each time step. If some valve is conducting, the corresponding element of the vector is declared as ″1″, otherwise the element is declared as ″0″. The nine possible states are summarized in Table 1.

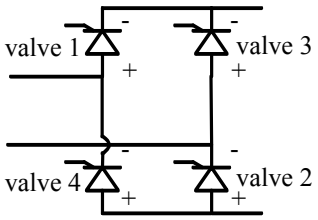

Fig. 3. Line commutated single-phase bridge inverter

Table 1. Possible states of ***S***

Valve No.	State vector **S**								
1	1	1	0	0	0	1	1	1	0
2	1	1	1	1	0	0	0	1	0
3	0	1	1	1	1	1	0	0	0
4	0	0	0	1	1	1	1	1	0

According to Table 1, commutation is included in the inverter model as it is shown at the second, fourth, sixth and eighth columns. The third and seventh columns do not correspond to real situations but they have been introduced for the necessity of the simulation. Finally, the ninth column presents a non-conducting situation, which appears in a non-continuous conduction operation of the inverter. The states of the vector **S** are a function of either only the system outputs or the system outputs and the commands of the control system.

2.3. Transformer model

For the representation of the transformer, the geometrical transformer model that is presented in [6] is used. This transformer model takes into account the magnetic core structure as well as the non-linearity of the core material. In particular, this model is based on the decoupling and the direct solution of the electric and magnetic circuits on the level of state equations.

Suppose the single-phase transformer shown in Fig. 4 where v_1 and v_2 are the voltages at the transformer terminals, i_1 and i_2 are the windings currents, ψ_1 and ψ_2 the flux linkages, L_1 and L_2 are the leakage inductances, r_1 and r_2 are the windings resistances at the primary and the secondary side, respectively. In Fig. 5 the magnetic circuit of the transformer core is shown where Φ the core flux, F is the total magnetomotive force due to the windings currents, R_m is the magnetic reluctance and f_{Rm} is the magnetic potential.

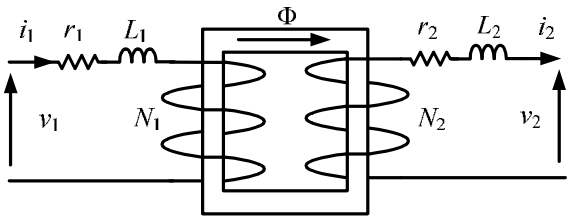

Fig. 4. A single-phase core-type transformer

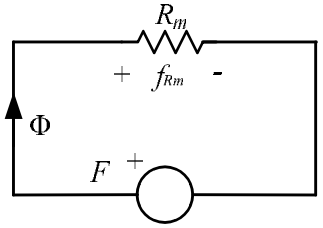

Fig. 5. The magnetic circuit of the magnetic core of the transformer in Fig. 4

According to [6], the coupling between the transformer's windings is represented by the incremental inductance matrix $\mathbf{L_d}$. The matrix $\mathbf{L_d}$ is symmetrical, it's diagonal elements represent the incremental self-inductances while the non-diagonal elements represent the incremental mutual-inductances of the windings.

In order to determine the matrix $\mathbf{L_d}$ one has to derive the differential equation of the magnetic flux in terms of the time derivatives of the windings currents i_1 and i_2 (Fig. 4). To this end, the time derivative of the core flux is written as

$$\frac{d\Phi}{dt} = \frac{\partial \Phi}{\partial f_{Rm}} \frac{\partial f_{Rm}}{\partial F} \frac{dF}{dt} \tag{6}$$

The time derivative of the magnetomotive force F is

$$\frac{dF}{dt} = N_1 \frac{di_1}{dt} - N_2 \frac{di_2}{dt} \tag{7}$$

Moreover, the partial derivative of the magnetic potential f_{Rm} with respect to the magnetomotive force F is

$$\frac{\partial f_{Rm}}{\partial F} = 1 \tag{8}$$

In [6] it is proved that

$$\frac{\partial \Phi}{\partial f_{Rm}} = G_{md} \tag{9}$$

where $G_{md} = \mu_d A_c / L_c$ is the incremental magnetic conductance, A_c is the cross section at the magnetic core and L_c is the mean length of the magnetic lines of the core. The term μ_d is the incremental magnetic permeability and is defined as $\mu_d = db/dh$ where b is the magnetic flux density and h is the magnetic field strength of the core. By substituting (7), (8) and (9) into (6) the differential equation of the magnetic flux is written as

$$\frac{d\Phi}{dt} = N_1 G_{md} \frac{di_1}{dt} - N_2 G_{md} \frac{di_2}{dt} \tag{10}$$

The time derivatives ψ_1 and ψ_2 of the windings are written in terms of the time derivative of the magnetic flux Φ as

$$\frac{d}{dt}\begin{bmatrix} \psi_1 \\ \psi_2 \end{bmatrix} = \begin{bmatrix} N_1 \\ -N_2 \end{bmatrix} \frac{d\Phi}{dt} \tag{11}$$

By substituting (10) into (11) the matrix $\mathbf{L_d}$ is derived and the result is

$$\mathbf{L_d} = \begin{bmatrix} N_1^2 G_{md} & -N_1 N_2 G_{md} \\ -N_1 N_2 G_{md} & N_2^2 G_{md} \end{bmatrix} \tag{12}$$

The electrical equations of the transformer in Fig. 4 are derived using the incremental self and mutual inductances in (12) and in matrix form are

$$\begin{bmatrix} v_1 \\ v_2 \end{bmatrix} = \begin{bmatrix} r_1 & 0 \\ 0 & r_2 \end{bmatrix} \begin{bmatrix} i_1 \\ i_2 \end{bmatrix} + \begin{bmatrix} L_1 + N_1^2 G_{md} & -N_1 N_2 G_{md} \\ -N_1 N_2 G_{md} & L_2 + N_2^2 G_{md} \end{bmatrix} \begin{bmatrix} \frac{di_1}{dt} \\ \frac{di_2}{dt} \end{bmatrix} \tag{13}$$

The inclusion of the hysteresis loop of the core material is accomplished using the Jiles-Atherton model. Specifically, using the fundamental equation

$$b = \mu_0 (h + M) \tag{14}$$

where μ_0 is the permeability of the free space and M is the magnetization of the core, the incremental permeability μ_d is given by

$$\mu_d = \mu_0 \left(1 + \frac{dM}{dh}\right) \tag{15}$$

The term dM/dh is the sum

$$\frac{dM}{dh} = \frac{dM_{rev}}{dh} + \frac{dM_{irr}}{dh} \tag{16}$$

where M_{rev} is the reversible magnetization and M_{irr} is the irreversible magnetization. According to the Jiles-Atherton model

$$\frac{dM_{irr}}{dh} = \frac{M_{an} - M_{irr}}{k\delta - a_1 (M_{an} - M_{irr})} \tag{17}$$

$$\frac{dM_{rev}}{dh} = c\left(\frac{dM_{an}}{dh} - \frac{dM_{irr}}{dh}\right) \tag{18}$$

where the term M_{an} is the anhysteretic magnetization, the parameters a_1, a_2, c and k are constants for the material being used, M_s is the saturation magnetization and the directional parameter δ is ± 1 and depends on the sign of dh. In terms of h, M_{an} is expressed by the modified Langevin equation

$$M_{an}(h) = M_s \left[\coth\left(\frac{h + a_1 M}{a_2}\right) - \frac{a_2}{h + a_1 M}\right] \tag{19}$$

The term dM_{an}/dh in (18) can be derived by differentiation of (19).

In order to follow the trajectory of the core material on the b-h plane, the quantities M_{rev}, M_{irr} and h have to be calculated. Hence, besides (10) the following differential equations are also required

$$\frac{dh}{dt} = \frac{1}{\mu_d A_c} \frac{d\Phi}{dt} \tag{20}$$

$$\frac{dM_{rev}}{dt} = \frac{dM_{rev}}{dh} \frac{dh}{dt} \tag{21}$$

$$\frac{dM_{irr}}{dt} = \frac{dM_{irr}}{dh} \frac{dh}{dt} \tag{22}$$

In this work, the typical hysteresis loop shown in Fig. 6 for a Fe-Si material is used according to [7].

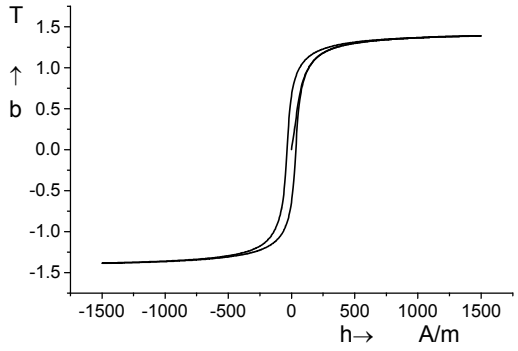

Fig. 6. Hysteresis curve for M_s= 1.146 10^6 A/m, α_1 = 1.3 10^{-4}, k = 99 A/m, α_2 = 59 A/m *and* c = 0.55

3. System modeling

The above-mentioned models for the main components of the system are mathematically combined into a system model for the presentation of the state equations for the grid connected PV system shown in Fig. 7.

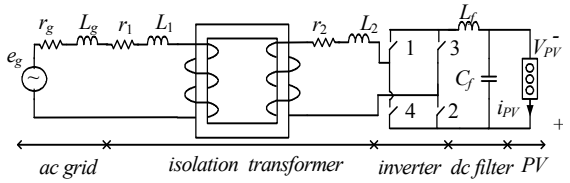

Fig. 7. Grid connected PV system

For example, suppose that the inverter is at a conduction mode where valves ″1″ and ″2″ are closed and valves ″3″ and ″4″ are open as shown in Fig. 8. Then, the vector **S** = [1 1 0 0]. In this case, the state variables of the electrical part of the system are the loop current i_1 at the primary side of the transformer, the loop current i_2 at the secondary side of the transformer and the voltage v_c at the capacitor terminals. Then, the equations of the electrical part of the system are

$$\begin{bmatrix} e_g \\ 0 \\ 0 \end{bmatrix} = \begin{bmatrix} r_g + r_1 & 0 & 0 \\ 0 & r_2 & -1 \\ 0 & r_{dn} & 1 \end{bmatrix} \begin{bmatrix} i_1 \\ i_2 \\ v_c \end{bmatrix} +$$

$$\begin{bmatrix} L_g + L_1 + N_1^2 G_{md} & -N_1 N_2 G_{md} & 0 \\ -N_1 N_2 G_{md} & L_f + L_2 + N_2^2 G_{md} & 0 \\ 0 & 0 & C_f r_{dn} \end{bmatrix} \begin{bmatrix} \frac{di_1}{dt} \\ \frac{di_2}{dt} \\ \frac{dv_c}{dt} \end{bmatrix} \quad (23)$$

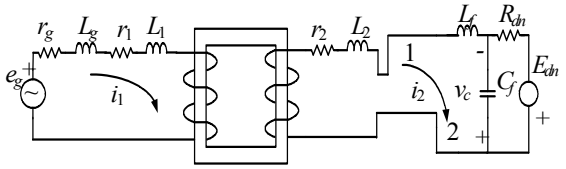

Fig. 8. System topology for **S** = [1 1 0 0]

In the case where **S** = [1 1 1 0], which means that the valves ″1″ , ″2″ and ″3″ are closed an extra loop arises at the ac side of the inverter. This leads to a different set of state equations and the number of state variables is increased to five. Thus, it is obvious that nine sets of state equations are employed and according to the value of the state vector the proper set is selected for integration in each time step.

4. Simulation results

Based on the proposed system model, simulation studies have been conducted for the John F. Long PV System [1]. System performance for insolation 400 W/m^2, 550 W/m^2 and 1000W/m^2 is shown in Fig. 9 and in Fig. 10, for the transient and the steady state, respectively, using the data shown in Table 2.

Table 2. Data for the simulation

ac Grid	
Resistance [mΩ]	23.6
Inductance [mH]	0.12
Frequency [Hz]	60
RMS voltage [V]	240
Transformer	
Windings	
Resistance [mΩ]	85.601
Leakage inductance [μH]	307.155
Number of turns	160
Magnetic core	
Mean length path [cm]	87.43
Cross-section [cm^2]	70.383
Dc filter	
Inductance [mH]	25
Capacitance [mF]	3.3

In Fig. 11 and in Fig. 12, the measured and the predicted values for the harmonic content of the injected current into the ac grid is shown for insolation 550 W/m^2 and 400 W/m^2, respectively. Comparing these results, for instance, for the third harmonic, which dominates, the error between the measured and predicted value is about 15% (550 W/m^2) and 8% (400 W/m^2). Concerning the Total Harmonic Distortion (THD), the error is 12.6% (550 W/m^2) and 5.6%

(400 W/m^2).

5. Conclusion

The mathematical description of the system model shows the way in which the proposed transformer model can be used for the modeling of grid connected PV, wind or fuel cell systems. The basic concepts of simulation are the same regardless of the switching pattern of the converter's electronics valves (e.g. PWM). The predicted values, for the specific system, present good agreement with the measured values and thus, the system model is a suitable tool for such studies. Moreover, the proposed system model can be used to sensitivity analysis on various design parameters for improvements during the design stage.

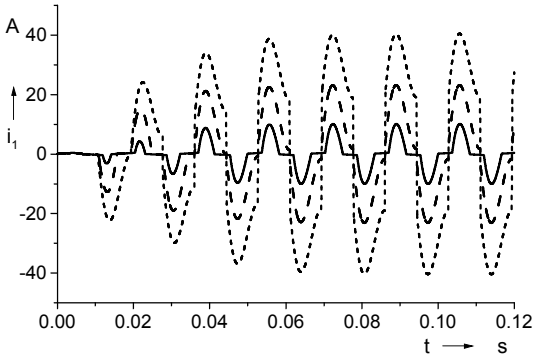

Fig. 9. Waveforms of the injected current into the ac grid for insolation 400 W/m^2 *(solid line),* 550 W/m^2 *(dashed line) and* 1000 W/m^2 *(sort-dashed line)*

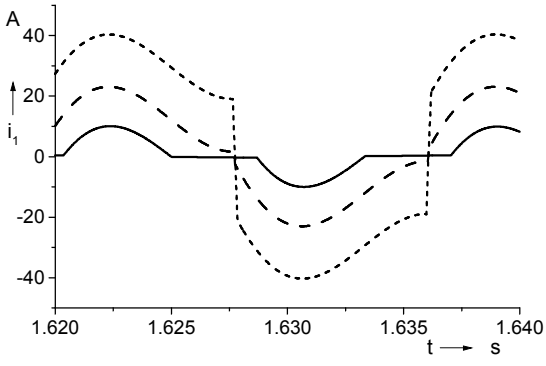

Fig. 10. Waveforms of the injected current into the ac grid for insolation 400 W/m^2 *(solid line),* 550 W/m^2 *(dashed line) and* 1000 W/m^2 *(sort-dashed line)*

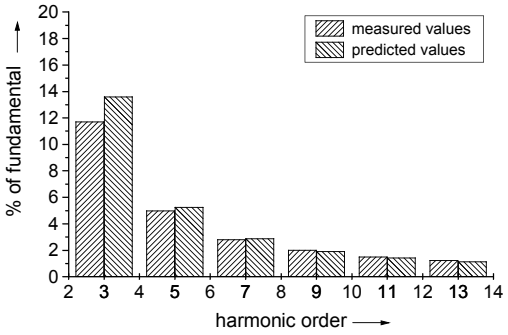

Fig. 11. Harmonic content of the injected current for isolation 550 W/m^2

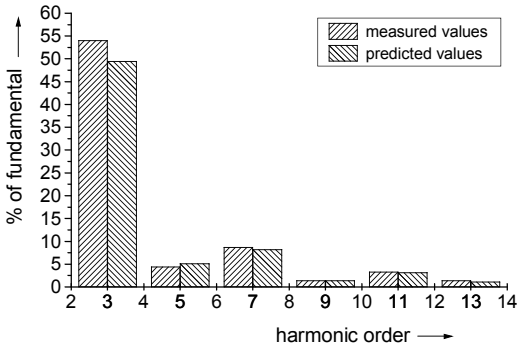

Fig. 12. Harmonic content of the injected current for isolation 400 W/m^2

6. Bibliography

[1] Mc Neill B., Mizra M.: *Estimated Power Quality for Line Commutated Photovoltaic Residential System*, IEEE Trans. Power Ap. an Systems, Vol. PAS-102, No. 10, pp. 3288-3295, Oct. 1983

[2] Campen G. L.: *An analysis of the harmonics and power factor effects at a utility intertied photovoltaic system*, IEEE Trans. Power Ap. and Systems, vol. PAS-101, No. 12, pp. 4632-4639, Dec. 1982

[3] Dugan R. C., Jewell W. T., Roesler D. T.: *Harmonic and reactive power from line-commutated inverters in proposed photovoltaic subvision*, IEEE Trans. Power Ap. and Systems, Vol. PAS-102, No. 9, pp3205-3211, Sept. 1983

[4] Zacharias Th., Milias-Argitis J., Makios V.: *First-order circuits driven by a photovoltaic generator*, Solar Cells, Vol. 31, pp. 57-75, 1991

[5] Milias-Argitis J., Zacharias Th.: *Transient phenomena of rlc circuits – The photovoltaic input*, Solar Energy Materials & Solar Cells, Vol. 55, pp. 363-378, 1998

[6] Theocharis A. D., Milias-Argitis J., Zacharias Th.: *Single-phase transformer model including magnetic hysteresis and eddy currents*, Electrical Engineering, vol. 9, no. 3, pp. 229-241, February 2008

[7] Thomas D. W. P., Paul J., Ozgonenel O.,

Christopoulos C.: *Time-domain simulation of non-linear transformers displaying hysteresis*, IEEE Trans. on Magn., vol. 42, pp. 1821-1827, July 2006

Authors

Theocharis Andreas, PhD Candidate,
e-mail: theoxar@ece.upatras.gr
Zacharias Thomas, Assistant Professor,
e-mail: zaxarias@ece.upatras.gr
Tsanakas Dimitrios, Professor,
e-mail: D.K.Tsanakas@ece.upatras.gr
Milias-Argitis John, Associate Professor,
e-mail: milias@ece.upatras.gr
University of Patras,
Department of Electrical and Computer Engineering,
Patras, 26500 Rion, Greece